*Article*

# DETER-R: An Operational Near-Real Time Tropical Forest Disturbance Warning System Based on Sentinel-1 Time Series Analysis

Juan Doblas *[ID], Mariane S. Reis [ID], Amanda P. Belluzzo [ID], Camila B. Quadros [ID], Douglas R. V. Moraes [ID], Claudio A. Almeida [ID], Luis E. P. Maurano [ID], André F. A. Carvalho [ID], Sidnei J. S. Sant'Anna [ID] and Yosio E. Shimabukuro [ID]

Earth Observation and Geoinformatics Division (DIOTG), National Institute for Space Research (INPE), São José dos Campos 12227-010, Brazil; mariane.reis@inpe.br (M.S.R.); amanda.belluzzo@inpe.br (A.P.B.); camila.quadros@inpe.br (C.B.Q.); douglas.moraes@inpe.br (D.R.V.M.); claudio.almeida@inpe.br (C.A.A.); luis.maurano@inpe.br (L.E.P.M.); andre.carvalho@inpe.br (A.F.A.C.); sidnei.santanna@inpe.br (S.J.S.S.); yosio.shimabukuro@inpe.br (Y.E.S.)
* Correspondence: juan.doblas@inpe.br

**Abstract:** Continuous monitoring of forest disturbance on tropical forests is a fundamental tool to support proactive preservation actions and to stop further destruction of native vegetation. Currently most of the monitoring systems in operation are based on optical imagery, and thus are flaw-prone on areas with frequent cloud cover. As this, several Synthetic Aperture Radar (SAR)-based systems have been developed recently, aiming all-weather disturbance detection. This article presents the main aspects and the results of the first year of operation of the SAR based Near Real-Time Deforestation Detection System (DETER-R), an automated deforestation detection system focused on the Brazilian Amazon. DETER-R uses the Google Earth Engine platform to preprocess and analyze Sentinel-1 SAR time series. New images are treated and analyzed daily. After the automated analysis, the system vectorizes clusters of deforested pixels and sends the corresponding polygons to the environmental enforcement agency. After 12 months of operational life, the system has produced 88,572 forest disturbance warnings. Human validation of the warning polygons showed a extremely low rate of misdetections, with less than 0.2% of the detected area corresponding to false positives. During the first year of operation, DETER-R provided 33,234 warnings of interest to national monitoring agencies which were not detected by its optical counterpart DETER in the same period, corresponding to an area of 105,238.5 ha, or approximately 5% of the total detections. During the rainy season, the rate of additional detections increased as expected, reaching 8.1%.

**Keywords:** time series analysis; forest monitoring; SAR; Sentinel-1

## 1. Introduction

The $CO_2$ emissions due to the destruction of tropical forests sum up to 5.4 Gt $CO_2$e yr$^{-1}$, which is the double of the annual emissions associated to the removal of the remainder of the global forest formations [1]. New studies show that the critical role of the tropical forest as the biggest sink of global greenhouse gases, with an annual removal of approximately 7.0 Gt $CO_2$e yr$^{-1}$ [1], is endangered due to deforestation and climate change [2]. Despite the multiple initiatives to reduce deforestation, and the growing global public awareness, the annual tree cover loss is constantly rising since the year 2000, reaching 12 million hectares in 2020 [3]. In these circumstances, near real-time (NRT) forest disturbance detection systems, which can be defined as a collection of algorithms and procedures able to identify tree loss or disturbance, on a periodic (monthly, weekly or even daily) basis, become a key aspect of deforestation reduction initiatives. This kind of system has been a crucial element to reinforce public policies that have led to significant deforestation rates decrease in Brazil [4], Peru [5] and more recently, in Indonesia [3].

In the Brazilian Amazon, the main NRT forest disturbance detection system in operation is the Near Real-Time Deforestation Detection System (DETER) [6]. DETER was developed to support the Brazilian Institute of the Environment and Renewable Natural Resources (IBAMA), as well as other associated agencies, in the inspection and control of Amazon deforestation and forest degradation. As such, one key aspect of DETER is its ability to alert priority disturbance events in near-real time with a low false-positive rate. DETER started issuing alerts in 2004, as part of the Action Plan for the Prevention and Control of Deforestation in the Legal Amazon (PPCDAm), which, coupled with the deployment of law-enforcement teams on the field and the delimitation of protected areas, contributed to a 83% decrease on deforestation rates from 2004 to 2012 [4]. Nonetheless, as DETER is based on optical data, it can be severely affected by the near constant cloud cover in certain parts of the Amazon in determined periods of the year, as the mean annual cloud cover on the Brazilian part of the biome is approximately 74% [7]. This is not a problem exclusive to DETER: a recent survey among NRT forest disturbance systems users pointed to cloud cover as the most important limiting factor to the effectiveness of these kind of systems [8].

Orbital active microwave sensors, namely Synthetic Aperture Radar (SAR) satellites, can help bridging the observational gap caused by cloud cover. SAR observations are not blocked (though they can be affected) by atmospheric conditions [9], and thus can continuously deliver land cover information on highly cloud-covered areas such as humid tropical forests. Following this premise, several operational or semi-operational NRT forest disturbance systems using data from the Advanced Land Observing System (ALOS)/Phase Array L-Band Synthetic Aperture Radar (PALSAR) or Sentinel-1A/B C-band sensors have been implemented in the last decade.

The first operational deforestation detection system based in orbital SAR information was the JICA-JAXA Forest Alert Warning System in the Tropics (JJ-FAST), an ALOS/PALSAR-based NRT system developed in 2016 by the Japanese Spatial Agency (JAXA), in cooperation with the Japan International Cooperation Agency (JICA). JJ-FAST has been continuously improved since its conception [10,11]. The last version of the system has 50-meter spatial resolution, a minimum mapping unit (MMU) of 2 ha, and a minimum revisiting time of 42 days.

Shortly after JJ-FAST implementation, the launching of European Space Agency (ESA) Sentinel-1 (S1) satellites (S1A and S1B), with publicly available images, triggered the development of several NRT systems based on their data. Here we will highlight the two main S1 based NRT systems operational nowadays, the RAdar for Detecting Deforestation (RADD) and the one from the French Centre d'Etudes Spatiales de la Biosphère (CESBIO).

The RADD system was originally developed at the Laboratory of Geo-information Science and Remote Sensing of the Wageningen University, while researching the suitability of the Bayesian classification and update approach to detect deforestation in near real-time using S1 time series [12]. RADD is operational over the entire tropics, using the Google Earth Engine (GEE, [13]) computing platform as the main computation engine, and the Global Forest Watch web infrastructure as the publishing framework [14]. It has a minimum mapping unit of 0.1 ha. The mean revisit time varies between 6 and 12 days.

Concomitantly, researchers from CESBIO developed a different approach to deforestation detection, based on the shadowing effect caused by forest removal. The researchers showed that detection of SAR shadows, by simple thresholding (i.e., flagging the pixels that have a backscatter intensity lower than the time-series mean), can accurately reveal deforestation patches boundaries [15]. The remainder of the deforested patch will be detected by lowering the original thresholding level. After a tropic wide research [16], an operational method based on S1 data has been developed and published, showing excellent results in south Asia [17]. As RADD, it has a minimum mapping unit of 0.1 ha, and a mean revisit time between 6 and 12 days.

All the previously presented systems use custom thresholds and detection parameters, defined after detailed heuristic research. As a matter of fact, the definition of the right thresholding technique and parameters is a key design step for every disturbance detection

system. Stricter thresholds will produce fewer false alarms, but can raise the false negative (or omission) rate until it reaches a point where important disturbances will not be detected. The CFAR (constant false alarm rate) standard can help to define the thresholding parameters, by letting the user of the system to define an a priori rate of false alerts. Although the CFAR paradigm is mainly used in SAR-based target detection systems, such as the Search for Unidentified Maritime Objects (SUMO) system [18], or more recently, to preprocess SAR images which will feed a machine learning target detector [19], it is also used as well in the image classification domain, for example to detect edges between different land-use parcels [20].

In [7] the authors developed a detector based on the premises of the CFAR standard, by studying the statistical distribution of the difference between the mean and the minimum incident angle-normalized backscattering coefficient ($\gamma_{VH}^0$) value associated to an Amazon-wide sample (n = 4 M) of intact-forest S1 time series. This procedure can be considered analogous to the procedure used to determine the background clutter model in the CFAR standard. The forest backscatter distribution proved to be normal, if computed over filtered images converted to decibel scale following the expression $\gamma_{VH}^0$ (dB) $= 10 \times log_{10}\gamma_{VH}^0$. The modelled distribution had a mean $m = -1.31$ dB and a standard deviation $\sigma = 0.35$ dB. Following this result, the authors proposed a forest disturbance detection method based on time-series thresholding, where the false alert ratio could be fixed by the setting of the number of standard deviations ($\sigma$) that determine the threshold below the mean of the forest minimum values. Fixing the threshold to $-2\sigma$, for instance, will theoretically equal to 97.4% of chances of not having a forest pixel detected as anomaly, or a CFAR of 2.6%. In this particular case, the value to be used as threshold will be $1.31 + 2 \times 0.35 = 2.01$ dB below the mean of the time series. Lower $\sigma$ values will decrease the threshold, decreasing the false alert ratio but can potentially increase the omission rate.

The results of this study [7] showed that backscattering thresholding, when applied in such an adaptive fashion, can overcome the results of the bayesian approach proposed in [12]. The advantage of the so-called Adaptive Linear Thresholding (ALT) method is the lack of assumptions about the non-forest backscattering distribution, which, due to its heterogeneity, can be a source of errors and false detections. These findings allowed the basis of the implementation of DETER companion system based on SAR data, called DETER-Radar (DETER-R), herein presented.

DETER-R is a fully automated NRT forest disturbance detection system based on S1 data. New images are treated and analyzed daily by an automated scripting scheme hosted in the GEE platform. After the automated analysis, the system vectorizes clusters of pixels flagged as forest disturbances and sends the corresponding polygons to the environmental enforcement agency. After running a prototype of the system from November 2020 to March 2021 over a set of five areas subject to special monitoring by the Brazilian National Institute for Space Research (INPE), the system was made operational, covering the Brazilian portion of the Amazon biome.

The main objective of this work is to describe DETER-R early and present routines, as well as the results generated in its prototype phase and after its first year of operation.

## 2. Materials

### 2.1. Project Area

A prototype of DETER-R was initially implemented over a set of 5 experimental areas, which were subject to special monitoring by INPE in the context of a frequent monitoring initiative called DETER-INTENSO (Intense DETER). These areas covered 458,000 km$^2$ and hosted most of the deforested areas in the year 2020 within the Brazilian Amazon. The operational version of the DETER-R system has as Area of Interest (AOI) the entire Brazilian Amazon Biome. It covers 4.21 million km$^2$, or 48.7% of the surface of Brazil. The system only takes in account changes affecting the forest cover within the AOI, which excludes already deforested areas up to year 2020, savanna, rivers, rocky outcrops, floodplains, and beach areas. The remaining area, which is being monitored by DETER-R, covers 2.81 million km$^2$,

or 66.7% of the entire AOI. The extension of both experimental and operational AOIs can be seen in Figure 1.
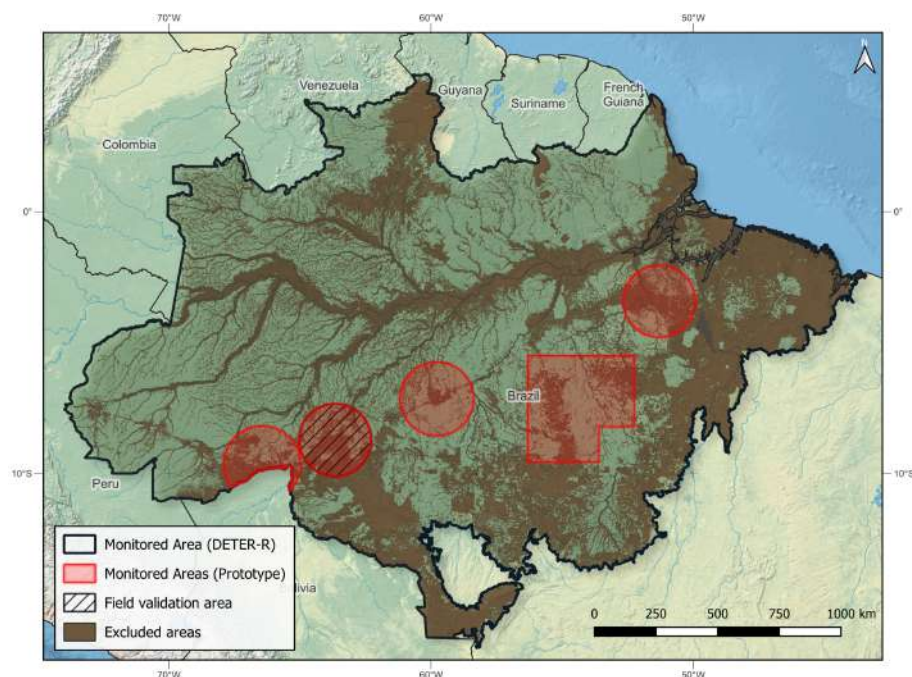


**Figure 1.** Area being monitored by the DETER-R system. The dark line represents the limit of the Amazon biome within the Brazilian borders. The brown-shaded areas represent regions belonging to the categories not monitored by the DETER-R system: already deforested areas, rivers, flood plains, savannas, beaches, and rocky outcrops. Red areas denote the experimental AOI where DETER-R prototype 2020 testing took place. The hatched circle shows the area of the field validation campaign.

*2.2. SAR Images*

The SAR images used on the DETER-R system are acquired by the Sentinel-1 (S1) satellites, and distributed free of charge by the European Space Agency (ESA). The GEE platform loads and preprocess the S1 data on a daily basis, converting the raw data to Ground Range Detected (GRD) images following these steps:

1. Orbit file correction: Updates orbit metadata with a restituted orbit file.
2. GRD border noise removal: Removes low-intensity noise and invalid data on scene edges.
3. Thermal noise removal: Removes additive noise in sub-swaths to help reduce discontinuities between sub-swaths for scenes in multi-swath acquisition modes.
4. Radiometric calibration: Computes backscatter intensity using sensor calibration parameters in the GRD metadata.
5. Terrain correction (orthorectification): Converts data from ground range geometry, which does not take terrain into account, to normalized backscatter coefficient using the Shuttle Radar Topography Mission (SRTM) 30 m Digital Elevation Models.

During the first year of operational life of the DETER-R system, a total 5111 Sentinel-1 images were treated, with a mean of 14 processed images/day. Around 80.0% of this total of images (4091 images) were acquired by the Sentinel-1A satellite, and the remainder by Sentinel-1B. We have recorded two main disruptions of the Sentinel-1 acquisition and processing pipelines:

1. During the first half of September 2021, issues with the image processing pipeline substantially reduced the availability of S1 images on the GEE platform. The images acquired during this period became available later in the same month.
2. On 23 December 2021, a power supply-related issue prevented switching on the Sentinel-1B SAR acquisition subsystem. Further investigation did not succeed on fixing the compromised systems. Although the satellite is still orbiting normally, its

operation is still stopped as of July 2022, and the future of the mission is uncertain. As a consequence of this incident, the mean number of images been made available over the DETER-R interest area dropped from 15.4 to 11.4 images/day.

Figure 2 illustrates the cadence of image processing over the first operational year of DETER-R system. The two mentioned incidents are clearly visible.
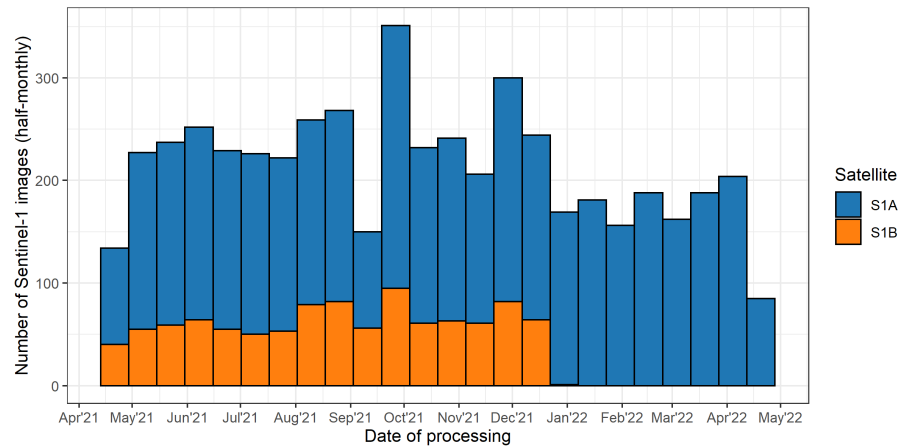


**Figure 2.** Cadence of images processing by the DETER-R system over its first operational year, illustrating the two main incidents affecting S1 images delivery by ESA: production gap in September 2021 and the stop of Sentinel-1B image production in January 2021.

### 2.3. Forest/Non-Forest Masks

In order to avoid the issuing of false deforestation warnings provoked by the natural variations of non-forested areas, the detection algorithm should be precisely informed of the extent of the evergreen forest. Normally, this information is provided as Forest/Non-Forest maps, also called Forest Masks. As it has been demonstrated in Sano et al. [21], no single mask can provide a precise estimate of the areas deprived of dense forest cover. As an important characteristic of DETER-R is the possibility to minimize the number of false warnings, we decided to built a non-forest mask by adding forest extent (or absence) information from different sources:

1.  deforestation map produced by the Program for Deforestation Monitoring in the Brazilian Legal Amazon (PRODES) [22]. This map is updated manually on DETER-R system every time the INPE/PRODES team issues an update. Normally this happens twice a year. The used map includes the residual (smaller than 6.25 ha) polygons which are not publicly available.
2.  INPE's Forest/Non-forest map, built by visual interpretation. This medium resolution map outlines regional non-forest compounds, such as Roraima's *lavrados.* This map is available at INPE's terrabrasilis website (http://terrabrasilis.dpi.inpe.br/ (accessed on 18 January 2022)).
3.  The German Aerospace Center (Deutsches Zentrum für Luft-und Raumfahrt - DLR) Forest/Non-Forest map, built automatically using mainly TerraSAR-X data [23]. This map contributes to capture small features such as isolated outcrops and savanna patches among rainforest regions.
4.  INPE's varzea (seasonally flooded) extent [24,25]. Including this dataset will exclude from monitoring scarcely deforested areas prone to false positives due to the effects on backscattering of seasonal flooding from monitoring.
5.  Flooded and beach areas mapped by the Brazilian Institute of Geography and Statistics (IBGE) [26]. This ancillary layer will avoid false positives arising from seasonally flooding and coastline tidal variations.

### 2.4. Validation Imagery

During the first year of operation, the warnings issued by DETER-R were validated by the visual interpretation of optical images. This step is not mandatory for the functioning of DETER-R and was executed to assess the system potential. The following sets of optical images were used:

1.  The Planet Basemaps Imagery, made available by the Norway's International Climate & Forests Initiative (NICFI) program. Monthly and semiannual mosaics with 3 m spatial resolution are used, both in the visual and normalized analytic modes.
2.  Sentinel-2 images, freely distributed by ESA with 10 m spatial resolution and hosted on the Amazon Web Services (AWS). The two most recent images for each location at the time of analysis are used.
3.  The Landsat images selected and pre-processed by the PRODES team in the previous year. Pre-processing includes the application of contrast and color composition Shortwave infrared (R)/Near-infrared (G)/Red (B). Images are used with original 30 m spatial resolution.

## 3. Methodology

The DETER-R system uses an hybrid parallel-pipeline processing paradigm. While the core of the system (the pixel-wise detection algorithm) runs over the parallel architecture of the GEE platform, the image selection and results of the detection are treated on a synchronous, sequential workflow. Figure 3 outlines the daily operational workflow of the DETER-R system. The workflow is triggered daily at 1 AM (Brasília Time-BRT) on a virtualized Linux box. The code used by DETER-R is open-source and can be downloaded at: https://github.com/jdoblas/DETER_R_AMZ (accessed on 15 March 2022).
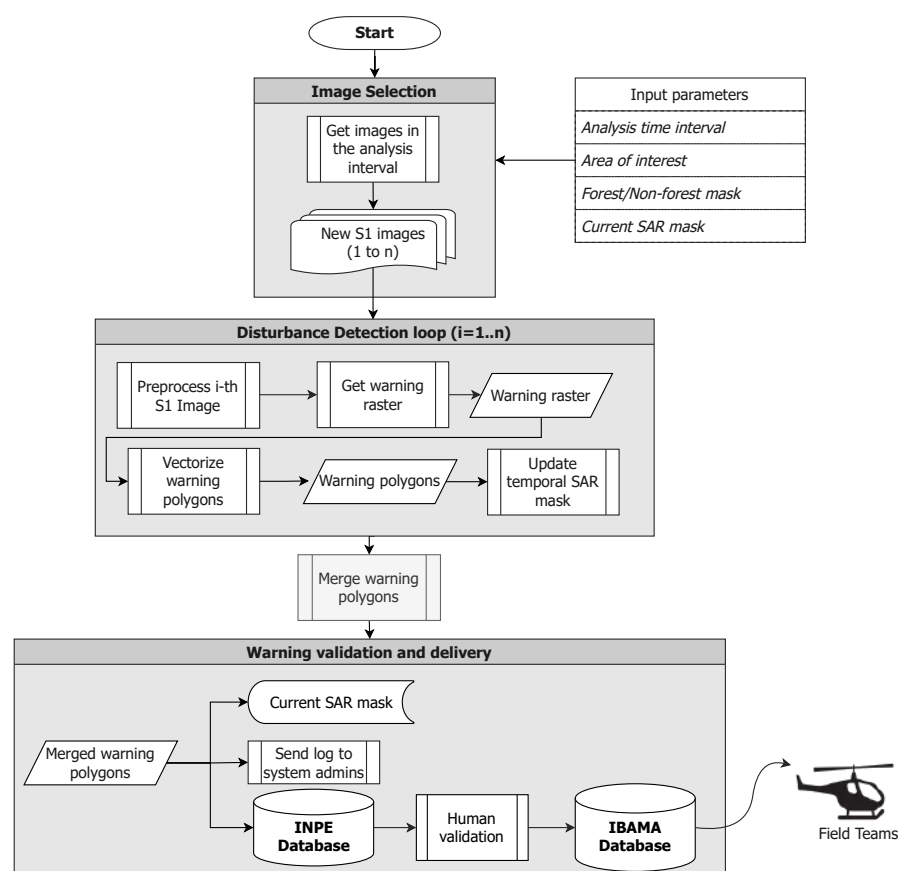


**Figure 3.** Flowchart depicting the daily operational routine of the DETER-R system.

### 3.1. Image Selection

The first step on the daily DETER-R routine is to select the images which were made available on the GEE platform during the selected time interval (normally the day before the execution).

### 3.2. Disturbance Detection

During the disturbance detection phase, all the images previously selected are processed in order to flag anomalous pixels. Clusters of flagged pixels will be vectorized and finally merged on a final warning dataset.

#### 3.2.1. Preprocessing

The goal of Sentinel-1 images preprocessing is (1) To correct the variation on backscatter intensity due to variations on the local incidence angle (LIA), (2) to reduce the speckle associated with the SAR signal, and (3) to reduce backscattering fluctuations due to seasonal variations of canopy moisture. To achieve this, the DETER-R system employs a standard processing sequence. As most of the AOI can be considered as being flat or, at most, hilly, LIA correction was performed following the expression:

$$\gamma^0 = \frac{\sigma^0}{cos\theta_i} \tag{1}$$

where $\sigma^0$ represents the normalized backscatter coefficient, $\theta_i$ the local incidence angle (LIA) and $\gamma^0$, known as gamma naught, is the backscattering coefficient normalized by the incidence angle. Disturbance detection in mountainous areas should follow a more complex procedure than the one applied here, such as the one recently proposed in [27].

Regarding speckle reduction, we decided to apply two different filters sequentially: a temporal filter (Quegan&Yu), and a spatial filter (Refined Lee $7 \times 7$ filter). The temporal filter [28] is applied to a given SAR image by collecting $M$ images acquired on the same location, and then applying the following expression:

$$J_k = \frac{\langle I_k \rangle}{M} \sum_{i=1}^{M} \frac{I_i}{\langle I_i \rangle} \tag{2}$$

where $J_k$ ($k \in [1, M]$) is the k-th filtered image, $M$ the total number of collected images, $I_i$ the intensity value of the image $i$, and $\langle I_k \rangle$ and $\langle I_i \rangle$ are the *expected* values of the image being filtered and the collected images, respectively. The expected value is computed by applying a simple spatial filter (in our case, a $5 \times 5$ box-car filter) to the corresponding image.

As specified in [28], it is advisable to apply a spatial filter to the results of the temporal filter. After systematic testing [29], we choose to apply a refined version [30] of the original Lee filter [31], due to its ability to preserve and enhance edge features in the input images.

Seasonal variations of the S1 backscattering signals due to variations on canopy moisture, the presence of intercepted rain and forest fragmentation have been investigated recently [32–34]. Here we have applied a harmonic stabilization technique, as described in [12], which constitutes an efficient and fast way of controlling this seasonality. To compute the stabilized value of an image at a given location, the algorithm: (1) applies an harmonic regression to fit a sinusoidal function to the backscattering time series in this location, (2) computes the difference between the original time series and the harmonic function, and (3) adds the median of the whole time series to the difference obtained in (2).

#### 3.2.2. Computation of Warning Rasters

The time series forest disturbance detection method applied is analogous to the ALT method proposed in [7]. It is based on the comparison of the backscatter value of a given set of filtered images (detection collection) with the median value of the backscatter values of the images acquired beforehand (learning collection). For a given image being evaluated, the detection collection comprises all the images acquired in the previous two months,

including the analyzed image itself. The learning collection will comprise the images acquired in the three years before the beginning of the learning collection. Any pixel of the detection collection with a difference value below a given threshold $t$ will be flagged as potential disturbed pixel. For a given image $k$ belonging to the detection collection, any pixel at a location $(x, y)$ that verifies the expression (3) will be flagged:

$$\left\langle \gamma_{VH}^0(x, y) \right\rangle_k - m_l(x, y) + t(x, y) < 0 \tag{3}$$

where $\left\langle \gamma_{VH}^0(x, y) \right\rangle_k$ is the backscattering value of a image $k$ of the filtered detection collection, $m_l(x, y)$ the median value of the backscattering of the learning collection, both expressed in dB, and $t(x, y)$ the chosen threshold value at this particular location. It is worth noting that the learning collection images are not being filtered, as the number of images ensure that the computed median value will be almost noiseless.

Figure 4 illustrates the steps followed on this particular phase of the system.
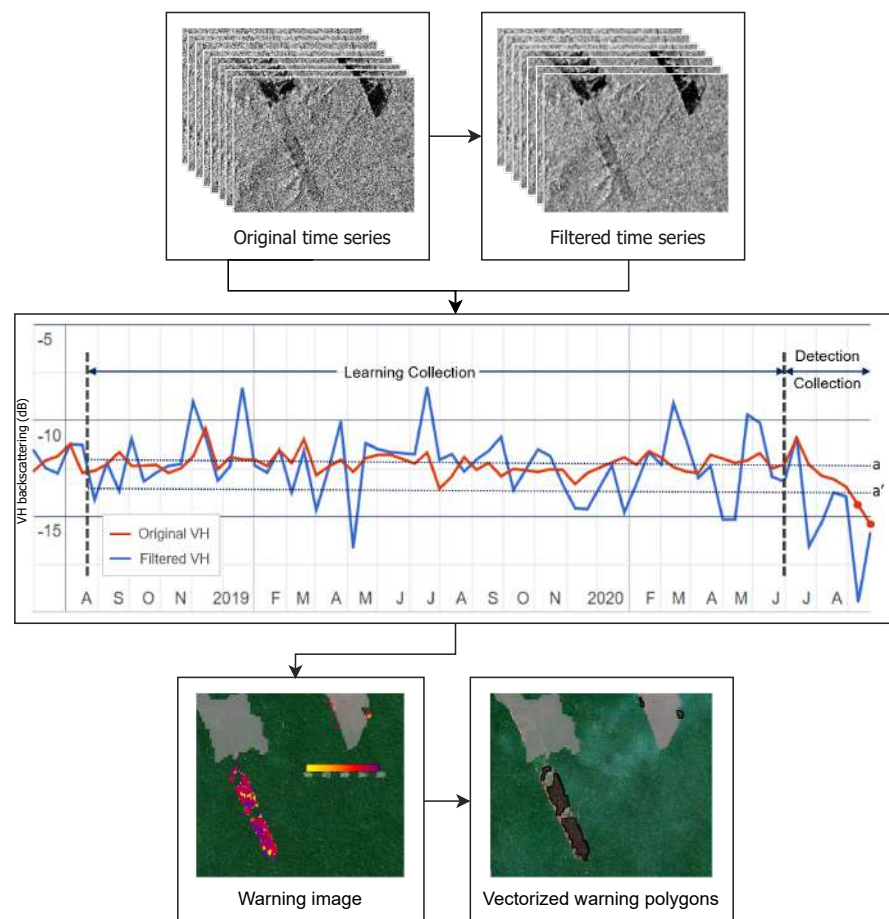


**Figure 4.** Detail of the warning detection procedure. Dotted lines a and a' denotes the median value of the learning collection and the threshold value for a particular location, respectively. The red dots correspond to samples below the threshold, which will be flagged. Two flagged values on the detection collection implies on a confirmed detection.

One of the most important aspects of the DETER-R system is the use of ancillary information on past deforestation to modify the detection threshold, trying to mimic the human interpreter behaviour, which will mistrust any deforestation alert on remote areas where man-made deforestation is improbable.

In order to quantify the probability of deforestation as a function of the proximity to previous deforestations, we have computed the distance from every deforestation polygon centroid mapped by the PRODES system to the previous year closest polygon, from 2016 to

2019. This procedure generated a probability function that was modeled with the help of the R library *fitdistplus* [35] as being a logistic distribution of $log_{10}(distance)$, with parameters location $\mu = 2.40633$ and scale s = 0.29973. Figure 5 shows the results of this modelling. These results suggest that most (>90%) of the deforestation on the Brazilian Amazon biome happens within 1 km of previously deforested areas.
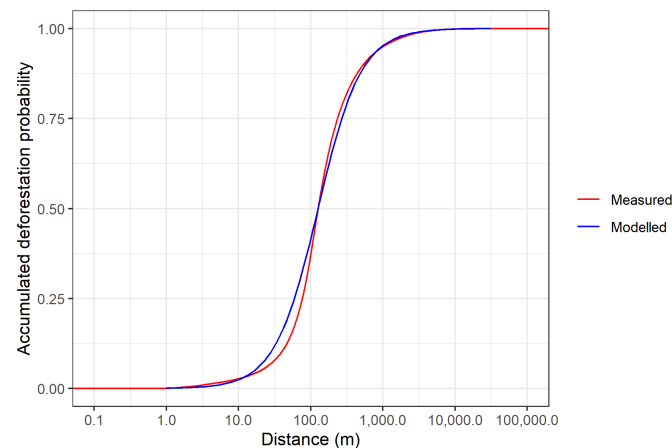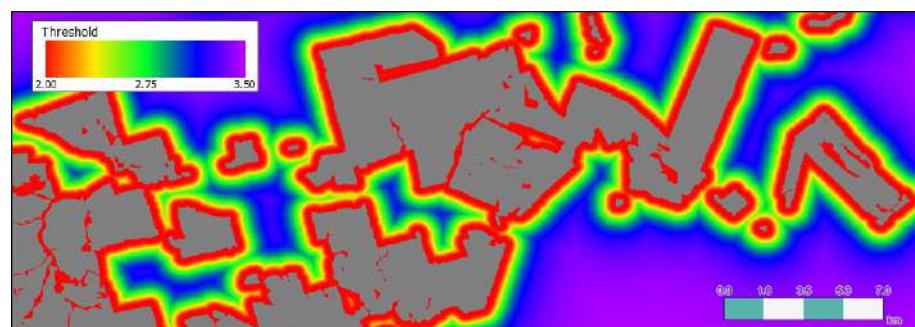


**Figure 5.** Accumulated probability of deforestation on the Brazilian Amazon, as a function of the distance to previous deforestations. The modelled distribution is a logistic distribution of $log_{10}(distance)$.

The results of this statistical study led us to change the deforestation detection methodology, which initially used a fixed threshold value, to a new approach, where the threshold to be applied to every pixel varies as a function of its euclidean distance to the previously deforested areas. The minimum value of this threshold will correspond to areas limiting with deforested areas, and the maximum value with correspond to the areas 10 km far from these areas. The value $t$ of the threshold in between will be computed following the previously modeled cumulative distribution function:

$$t(d; t_0; t_{max}; \mu, s) = d_0 + (t_{max} - t_0)\left(\frac{1}{2} + \frac{1}{2}\tanh(\frac{\log_{10}(d) - \mu}{2s})\right) \qquad (4)$$

where $d$ is the distance to the nearest deforestation, $t_0$ and $t_{max}$ are the thresholds corresponding to the minimum and maximum distances, and $\mu$ and $s$ are the distribution parameters previously found.

Figure 6 shows an example of the output of this procedure, as a spatially explicit threshold map.



**Figure 6.** Example of variable threshold map, built as a logistic accumulated probability function. Grey areas represent past deforestation. Notice how the threshold values increase with the distance to past deforestation.

### 3.2.3. Warning Vectorization and Filtering

After the previous detection step, the resulting warning image is vectorized. For every vectorized polygon, the algorithm will compute three parameters:

1.  Number of warnings: the mean value, across the polygon, of the total number of values below the threshold on the detection collection, computed for every pixel on the polygon.
2.  Day of change: The mode of the Julian day corresponding to the first perturbation on the detection collection.
3.  Intensity of change: median value of the difference between the threshold and the minimum value of the detection collection.

These polygons are filtered according to two parameters:

1.  Number of warnings: Polygon mean must be higher than 1. A value of 1 means that this polygon pixels were flagged only once, and the polygon should be discarded. This procedure mainly aims to remove the anomalies related to convection clouds, which provoke sudden and dramatic drops on backscattering [9].
2.  Size of the warning polygon: Polygons smaller than the system MMU will be discarded. Although theoretically this threshold can be fixed to values as low as one single pixel area, such a reduced MMU will raise the number of warnings caused by small-scale or spurious events associated with moisture variations [32] or speckle. Already existing S1-based detection systems [14,17] fix their MMU to values around 0.1–0.2 ha, to reduce the amount of false positives while allowing the detection of small deforested patches. In our case, after discussion with the system main users and stakeholders we decided to use a MMU of 1 ha, in order to encompass the main objectives of the environmental teams' field campaigns and their budgetary limitations.

The polygons that pass this filter are further classified into two forest disturbance classes, namely 'Low Intensity' and 'High Intensity', by thresholding the 'intensity of change' value. Polygons with the 'intensity of change' value equal or lower than the threshold are labeled as 'Low Intensity', and represent areas that have probably followed a forest degradation process, such as fires or initial slashing, but in which clear-cut events were not observed. Therefore, the remaining polygons, with 'intensity of change' higher than the threshold, are labeled as 'High Intensity' and correspond to areas of probable clear-cut deforestation with burning, as well as areas heavily burned/that have suffered several successive fires. At the initial phase of the project, the threshold was defined as 10.0 dB, based on the observation of sampled warnings. After the analysis of the first results and comprehensive data from the operational validation, this threshold was corrected to 7.0 dB in 17 June 2021.

### 3.2.4. Merging

Once all the selected Sentinel-1 images are processed, the corresponding vectorized warnings are merged and dumped to a PostGIS database. Normally, this will be the end of the automated detection cycle. Nevertheless, during the first year of DETER-R functioning it was decided to perform an visual validation procedure, which will be described in the next section.

### 3.3. Warnings Validation

The warnings issued in the previous step were validated on a daily basis by a team of interpreters linked to the project. This validation had three main objectives: (1) to calculate statistics of accuracy of the data obtained; (2) to eliminate detection errors and false alerts; and (3) to identify points to be improved in the system.

The validation process is illustrated in Figure 7. First, the warnings are compared to the deforestation polygons detected by the optical DETER [6]. DETER-R alerts with an overlap greater than 50% to optical DETER deforestation alerts are automatically validated as deforestation. A subset of the remaining warnings from DETER-R is then selected to be

validated based on the visual interpretation of the optical data described in Section 2.4. The 100 warnings with the largest area, and up to other 300 random warnings, are selected in this validation phase. Therefore, the interpreters validated up to 400 warnings/day, using an in-house web application [36], in the following classes:

1.  Recent Deforestation: complete and recent removal of the forest cover due to clear-cut or as the result of successive disturbance events. A deforestation process is considered recent if it occurred within the year of the PRODES project (August to July).
2.  Recent Degradation: partial loss of forest canopy and consequent exposure of soil and/or understory vegetation.
3.  Burnt areas: forested areas impacted by fire. It may or may not contain arboreal vegetation.
4.  Residue: old deforestation process, i.e., complete removal of the forest cover that can be detected in the images used by PRODES in the previous year.
5.  Water-flooded areas: previously forested areas that have been flooded or engulfed by river dynamics. This class was only considered from mid-June 2021. Early validated warnings of this class were labeled as Non-forest formations.
6.  Non-forest formations: recent alterations occurring in areas not originally covered by forests.
7.  False positive: forested areas with no detectable forest disturbances.
8.  Cloud: warnings that could not be assessed due to clouds in the optical images used for validation.
9.  No reference data: areas that could not be evaluated due to the absence of recent optical images at the validation time.
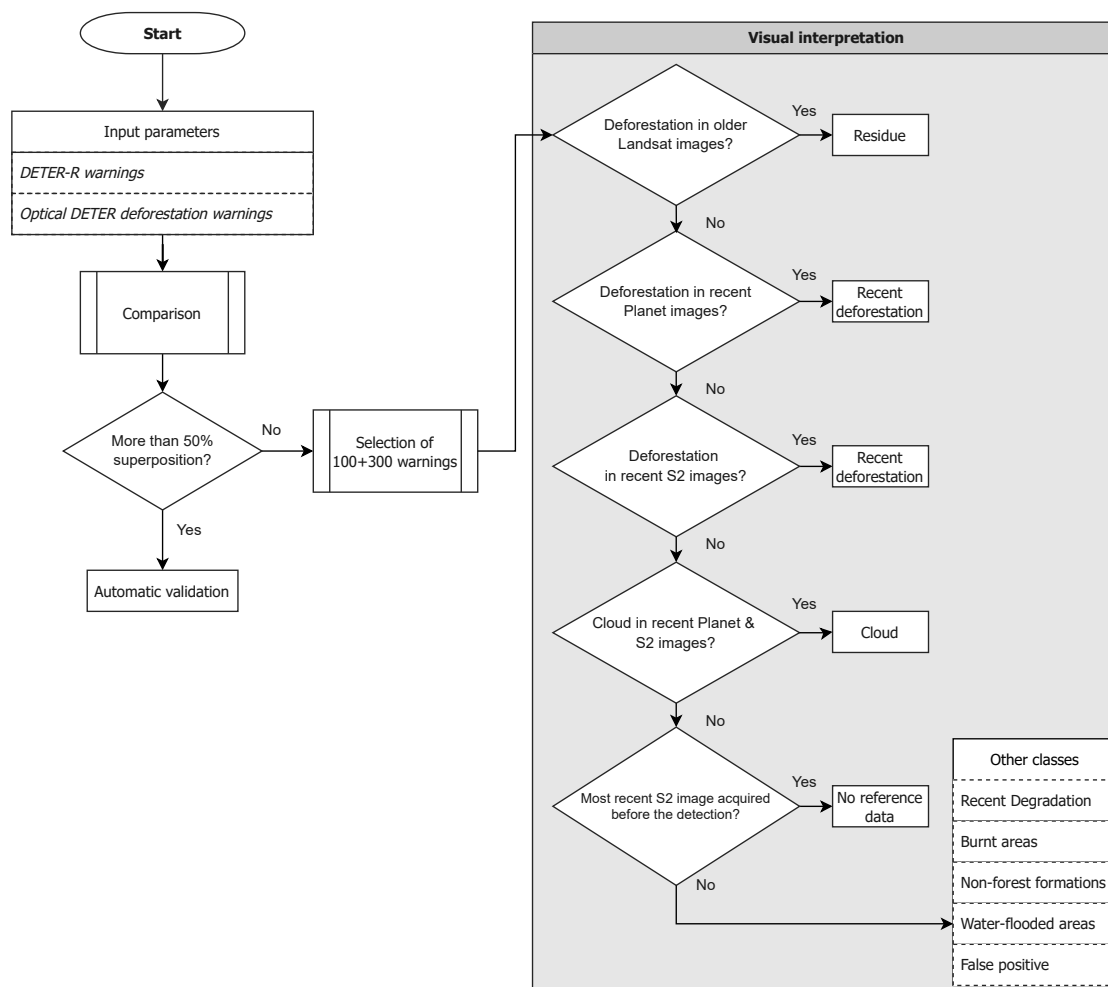


**Figure 7.** Flowchart of validation process.

The validated alerts were then used to calculate the system's accuracy. Alerts were tabulated according to the validated class, in four categories:

1.  Agreement: warnings of forest disturbances correctly detected as High/Low Impact.
2.  Minor disagreement: warnings of forest disturbances incorrectly detected as High/Low Impact.
3.  Major disagreement: warnings that do not correspond to forest disturbances.
4.  Not Evaluated: warnings that could not be evaluated.

The definition of each of the validation categories is illustrated in Table 1. We calculated the proportion of each validation category considering, separately, the number and the area of the validated warnings.

**Table 1.** Validation categories.

| Validation Class | Detection Class | |
| --- | --- | --- |
| | **High Intensity** | **Low Intensity** |
| Automatic (deforestation) | Agreement | Minor disagreement |
| Recent Deforestation | Agreement | Minor disagreement |
| Recent Degradation | Minor disagreement | Agreement |
| Burnt areas | Minor disagreement | Agreement |
| Residue | Minor disagreement | Minor disagreement |
| Water-flooded areas | Major disagreement | Major disagreement |
| Non-forest formations | Major disagreement | Major disagreement |
| False positive | Major disagreement | Major disagreement |
| Cloud | Not evaluated | Not evaluated |
| No reference data | Not evaluated | Not evaluated |

### 3.4. Warning Delivery

Alerts validated as 'Recent Deforestation', 'Residue', 'Cloud', and 'Not evaluated' are then sent automatically to the National Center for Monitoring and Environmental Information (CENIMA/IBAMA), via File Transfer Protocol (FTP), for further investigation on the field. These classes correspond to those that are either confirmed as deforestation by the operational validations, or those that could not be discarded as such. The protocol when using only S1 data (i.e., without the operational validation based on optical images) is to transfer the warnings issued as of 'High Intensity'. Currently, DETER-R data are not publicly available. Besides INPE and IBAMA, the Operations and Management Center of the Amazonian Protection System (CENSIPAM) also has access to the generated data.

## 4. Results

### 4.1. Preliminary Field Validation

During the month of November of 2020, a joint mission CENIMA/INPE overflew 100 randomly chosen warnings issued by the DETER-R prototype, around the region of Porto Velho (Rondonia State). The objective of the mission was to test the reliability of the warnings on an operational context. Another 170 preliminary warnings (with no second-image confirmation) were verified as well. Figure 8 shows the targets and the results of this validation mission.
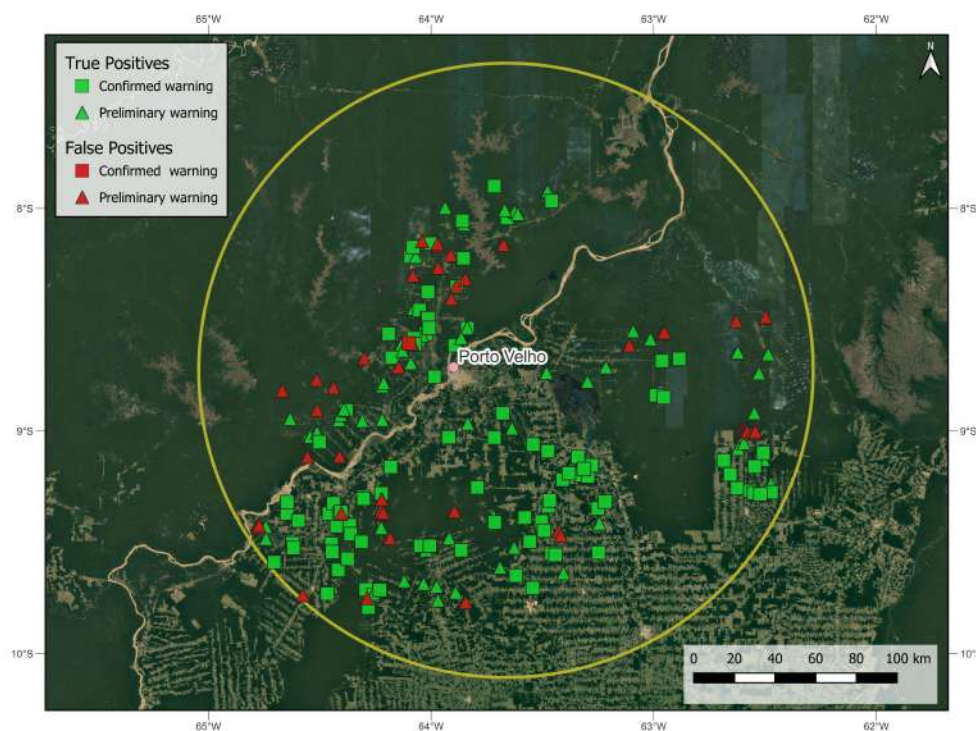
**Figure 8.** Detailed map of the field validation results. The outer yellow circumference corresponds to the limits of the monitored special area.

Results showed that 99 out of 100 of the inspected confirmed warnings corresponded to recently deforested areas. The preliminary warnings had a lower rate of success: 70% was confirmed, being the remainder false warnings provoked by convective clouds. These results stressed the need for two-image confirmation and the reliability of the confirmed warnings issued automatically by the system.
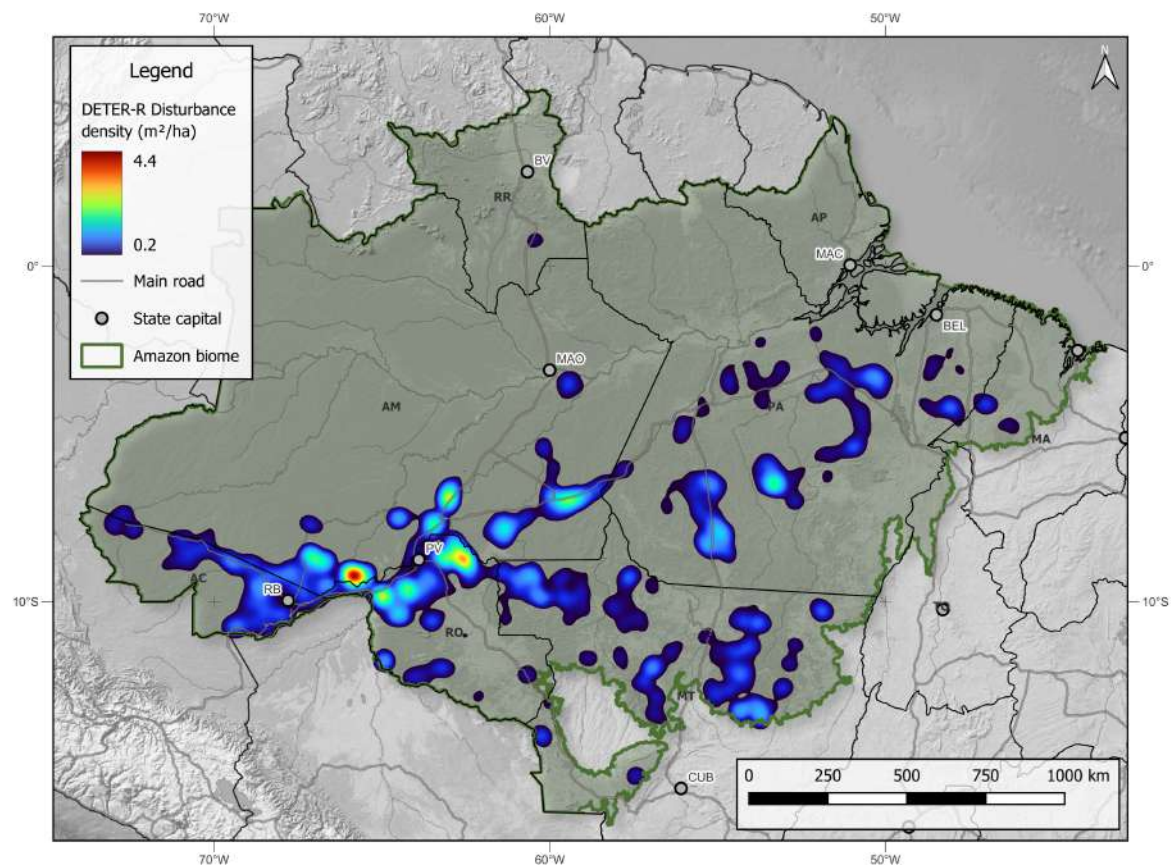
*4.2. Forest Disturbance Warnings*

The DETER-R system detected a total amount of 88,572 warning polygons through its first year of operation (from 21 April 2021 to 20 April 2022), which represents a mean detection rate of 242 warnings/day.

As expected, warnings were concentrated around the so-called 'arch of deforestation' (Figure 9). Meanwhile, some disturbance hotspots appear to penetrate further on previously preserved areas, such as the south of the Amazonas (AM) state, on its borders with Rondonia (RO) and Acre (AC). The analysis of the recent dynamics of deforestation in the Brazilian Amazon is out of the scope of this work. Interested readers may refer to [37].

Figures 10 and 11 show some examples of the detections carried out by the system. In these figures, the warnings are superimposed over optical Planet Labs images, for reference.

Temporally, the warnings were distributed unevenly during the year (Figure 12), being the central months of the year the most prolific on warnings. These results support the assumption that deforestation tasks are reduced during the wetter months of the year (November to March), which were months with reduced observations from the optical based systems.

DETER-R needs two anomalous SAR observations over a two-month S1 pre-processed time series to confirm a warning. This implies on a delay between the actual date of forest disturbance and the day the warning is issued to the institutions responsible for law enforcement and potentially other stakeholders. The time between the acquisition of the data and its availability on the GEE servers also adds up to this delay.

**Figure 9.** Heatmap of the forest disturbance warnings issued by the DETER-R system on its first year of operation. Disturbance density refers to the area in m² disturbed per hectare, integrated along a circular kernel of 50 km. For clarity purposes, areas with a disturbance density lower than 0.2 m²/ha were masked out.



(**a**) September'20      (**b**) September'21      (**c**) Warning polygons

**Figure 10.** Example of deforestation warnings issued by the DETER-R system in September 2021 near the city of Apui (AM), besides the BR-230 (Transamazônica) highway. In this case deforestation is linked to cattle-ranching. Satellite background true-color image by Planet Labs Inc.

(**a**) January'21        (**b**) April'22        (**c**) Warning polygons

**Figure 11.** Example of deforestation warnings issued by the DETER-R system inside the Kayapó Indigenous Territory, in the state of Pará. Clearings are caused by illegal sand and gold mining. Notice the small features not captured by the detection algorithm due to the Minimum Mapping Area constraint. Satellite background true-color image by Planet Labs Inc.
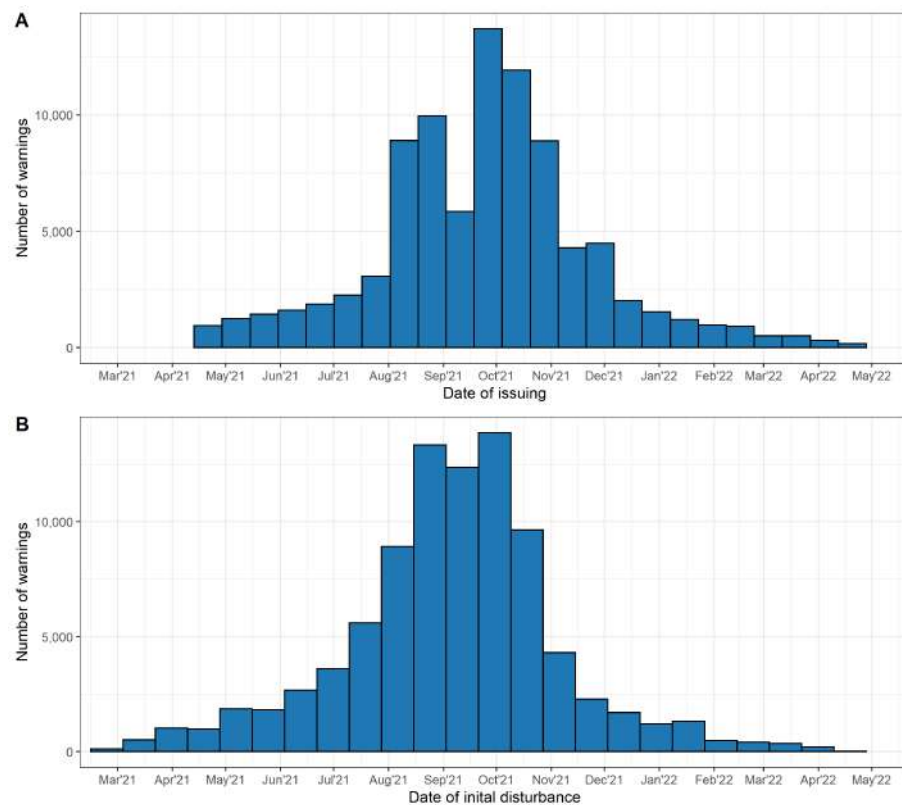


**Figure 12.** Timeline of the DETER-R detections. (**A**) The horizontal axis represents the date when the warning was issued (**B**) The horizontal axis represents the date of the detected disturbance.

After a year of regular operation, we have a mean issuing delay of 24 days, with a median value of 23 days. The maximum of the probability density distribution corresponds to 18 days (Figure 13). It is worth noting that the density distribution has a long right tail, instead of an expected symmetric, normal distribution. This asymmetry is probably due to the warnings issued after the late ingestion of some S1 images on the GEE platform, which can provoke delays of more than 60 days. Thus, we should expect a nominal issuing delay of 18 days during the normal operation of the system.
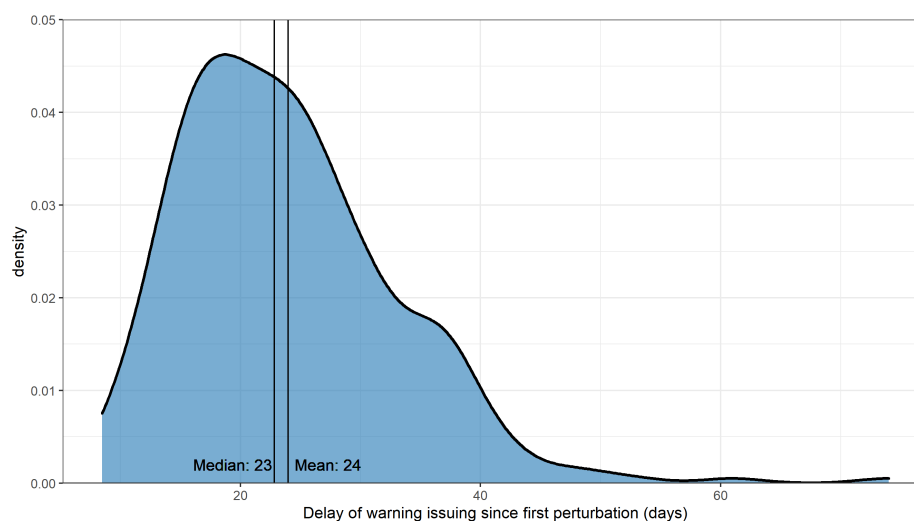
**Figure 13.** Density distribution of the issuing delay (the difference in days between the date of the actual forest disturbance and the date of the issuing of the corresponding warning).

### 4.3. Operational Validation

DETER-R was primarily designed to provide field teams with reliable forest disturbance information. As such, it is tailored to minimize Major disagreements, which are warnings that would probably waste field efforts. This characteristic is reflected in Table 2, that presents the results of the operational validation for the first year of DETER-R data. As can be seen, DETER-R achieves a low rate of Major disagreements, both considering the number and the area of the warnings. Furthermore, the major source of misdetections leading to Major disagreements occurred in areas of Non-forest formations, which can potentially be corrected using improved masks.

Around 96.7% of the issued warnings (97.6% of the detected area) were considered as valid (Agreement + Minor disagreement categories). Although a high proportion of the warnings has been automatically validated, DETER-R was capable to correctly detect 23,060 polygons of Recent Deforestation, corresponding to 77,899.3 ha of deforestation warnings that were not detected by its optical companion DETER at the emission date. In this sense, the existence of warnings validated as 'Residue' also show that DETER-R was capable to alert a deforestation event not previously registered either by DETER or PRODES, which are regarded as accurate systems.

There is a relative high confusion among 'High Intensity' and 'Low Intensity' classes, reflected in the existence of 23,237 warnings (27.2%)/67,380.2 ha (14.9%) of Minor disagreement. However, the majority of these disagreements come from areas misdetected as of 'Low Intensity', which are currently not of interest to field teams, so this confusion is not detrimental to the effectiveness of the system.

**Table 2.** Validated warnings between 21 April 2021 and 20 April 2022. The values in percentage are given in parentheses.

| Validation Class | Detected Polygons | | Detected Area (ha) | |
|---|---|---|---|---|
| | High Intensity | Low Intensity | High Intensity | Low Intensity |
| Automatic (deforestation) | **33,933 (39.7)** | *12,980 (15.2)* | **288,798.8 (63.9)** | *32,482.9 (7.2)* |
| Recent Deforestation | **23,060 (26.9)** | *6443 (7.5)* | **77,899.3 (17.2)** | *12,815.4 (2.8)* |
| Recent Degradation | *460 (0.5)* | **670 (0.8)** | *1214.0 (0.3)* | **1349.3 (0.3)** |
| Burnt areas | *1322 (1.5)* | **1859 (2.2)** | *17,550.6 (3.9)* | **5771.3 (1.3)** |
| Residue | *1580 (1.8)* | *462 (0.5)* | *2619.8 (0.6)* | *697.6 (0.2)* |
| Water-flooded areas [1] | 126 (0.1) | 11 (<0.1) | 170.5 (<0.1) | 20.1 (<0.1) |
| Non-forest formations [1] | 449 (0.5) | 194 (0.2) | 1535.0 (0.3) | 393.2 (0.1) |

**Table 2.** *Cont.*

| Validation Class | Detected Polygons | | Detected Area (ha) | |
|---|---|---|---|---|
| | High Intensity | Low Intensity | High Intensity | Low Intensity |
| False positive [1] | 224 (0.3) | 119 (0.1) | 434.7 (0.1) | 233.1 (0.1) |
| Cloud [2] | 467 (0.5) | 165 (0.2) | 3527.4 (0.8) | 360.0 (0.1) |
| No reference data [2] | 737 (0.9) | 319 (0.4) | 2997.1 (0.7) | 898.6 (0.2) |
| Agreement | 59,522 (69.6) | | 378,818.6 (82.7) | |
| Minor disagreement | 23,237 (27.2) | | 67,380.2 (14.9) | |
| Major disagreement | 1123 (1.3) | | 2786.5 (0.6) | |
| Not evaluated | 1688 (2.0) | | 7783.0 (1.7) | |

[1] Classes that led to Major disagreements. [2] Classes considered as Not evaluated. Note: Agreements are highlighted in bold font and Minor disagreements are highlighted in italic.

### 4.4. Delivered Warnings

During its first year of operation, DETER-R sent 83,332 forest disturbance warnings to IBAMA. From these, 33,096 warnings (39.7%) did not present a superposition of 50% or more to the warnings sent to IBAMA by the optical DETER in the same period. These values correspond to an area of 105,238.5 ha of forest disturbances alerted either first or only by DETER-R, or approximately 5% of the total area of warnings sent to IBAMA during the period. If we analyse only the rainy season, from November to March, this percentage increases to 8.1%. The distributions of the warnings of interest detected only by DETER-R is illustrated in Figure 14.
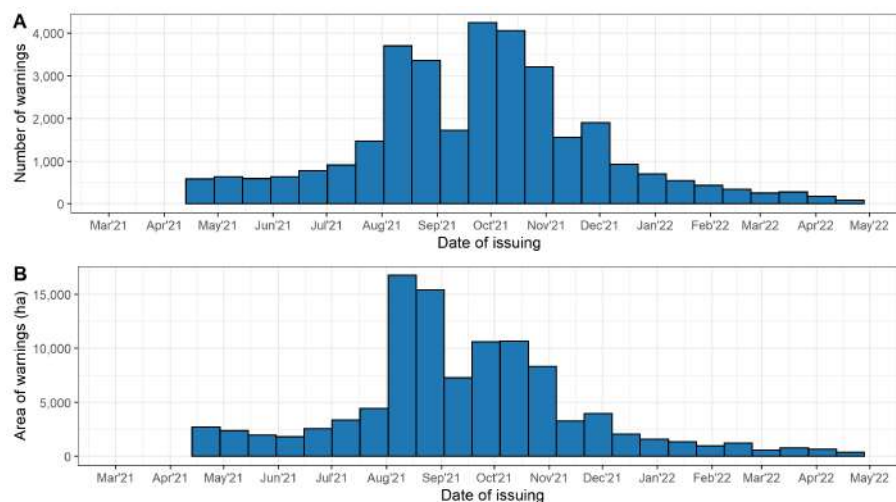


**Figure 14.** Timeline of DETER-R warnings not seen by the optical DETER in the same period sent to the Brazilian Institute of the Environment and Renewable Natural Resources (IBAMA) for field investigation (**A**) Number of warnings (**B**) Area of warnings.

## 5. Discussion

In this section, we will discuss the results obtained by DETER-R in its first year of operation in three main aspects: (1) Divergencies to other SAR based NRT systems in operation within the Brazilian Amazon; (2) System caveats, as identified in the present study; (3) Potential usefulness of the system to field enforcement teams.

### 5.1. Differences among DETER-R and Other Operational NRT Systems

Whereas general NRT systems aim to accurately detect most forest disturbances occurring in the AOI, with a given rate of misdetections allowed, DETER-R was tailored to assist field enforcement teams. As such, one fundamental premise of DETER-R is that it must issue no (or very few) false positives, to avoid costly displacements to non-

deforested areas, even at the cost of a higher rate of false negatives. Furthermore, the system was designed with a MMU fixed to 1 ha, since the field intervention teams will only be triggered to inspect medium to big-sized areas, due to operational and budgetary limits. These constraints led to a system with very low rate of misdetections, as suggested by the validation results. Expert-labeled validations evaluated Major disagreements to be 0.6% of the total detected area, while Minor disagreements, mainly caused by heavily burned or degraded areas, represent 14.6% of the total detected area. If we assume the Major disagreement to represent the misdetections of the DETER-R system, we can conclude that our system has a User's Accuracy of 99.4%. This rate can be compared with those presented in [38] (86.5%) over the Peruvian dense forests (GLAD system), 97.6% reported in [14] by the RADD system in the Congo basin, and 95.0% reported in [17] on its operational, S1-based system in South-Asia.

Regarding producer's accuracy, it is a known issue within DETER-R that this low rate of false positives leads to the omission of real warnings. In the parallel study conducted by Doblas et al. [39], the authors compared the performance of DETER-R to the previously cited SAR based NRT detection systems (CESBIO, JJ-FAST, and RADD), as well as the state of the art optical system GLAD-S2 [40]. This comparison showed that whereas all systems present User's Accuracies higher than 94%, only DETER-R achieved values comparable to GLAD-S2 (100%). Conversely, DETER-R achieved a poor Producer's Accuracy (around 50%) when compared to GLAD-S2 (85%). It roughly means that, while all the detections from DETER-R where true positives, half of the real deforestation warnings were omitted. Nonetheless, the Producer's Accuracy for DETER-R is higher than the one obtained by JJ-Fast (23%). Others SAR based systems presented higher values, ranging from 89% (CESBIO) to 92% (RADD).

The authors [39] also concluded that the methodology behind DETER-R can be adapted to improve the detection rate, at the price of a slight increase of the rate of false detections. For instance, they proposed an example of such a process, in which results of the tuned system are comparable to other SAR NRT detection systems, with User's Accuracy of around 98% and Producer's Accuracy around 90%.

*5.2. System Caveats*

As presented in Section 4.2, DETER-R warnings are issued with a nominal delay of 18 days and a mean delay of 24 days after the first perturbation, which, even if it is not optimal to guide rapid field incursions to stop deforestation processes, can allow for a intervention on cloudy areas not covered by standard optical NRT warning systems. We expect these delays to improve after the launching of the Sentinel-1C, scheduled for 2023. It is worth mentioning that the main source of detection delay is the actual need for redundancy while looking for time-series anomalies on a pixel-wise basis. One single anomalous backscattering value on the time series might be caused by the passage of a dense convection cloud [9] or by a transient, local perturbation of the canopy structure. Being so, neighbourhood-aware algorithms such as machine learning pattern recognition based on textural features and convolutional neural network-based deep-learning classification can be exploited to reduce or even eliminate the need for redundancy. Also, experimental techniques using ancillary precipitation data to mask storm-related SAR observations has been developed [41]. Until the date of writing of this article, no NRT system has been able to apply these kind of techniques on an operational basis, although approaches based on deep learning algorithms have shown promising results [42–44].

Regarding the results presented in Section 4.3, DETER-R presented 23,237 warnings evaluated as Minor disagreements, corresponding to 27.2% of the detected polygons and 14.9% of the detected area. As previously mentioned, these disagreements do not preclude the use of DETER-R for field validation efforts. Furthermore, we would like to highlight the relatively simple threshold method used to classify the level of impact of the warnings. To our knowledge, these classes are not easy to automatically separate using C-band SAR data due to the heterogeneity of the backscattering response to fire, drought or selective-logging degradation, as shown in [45].

*5.3. DETER-R Data as a Field Enforcement Tool*

So far, DETER-R has operated in a scientific capacity only, with the generated warnings not available to the public. Still, this system is supposed to run parallel to the optical DETER. Therefore, as important as the total amount of issued warnings, are the ones issued first/only by DETER-R, i.e., the warnings not previously detected by DETER and/or PRODES systems. In its first year of operation, DETER-R contributed with 105,238.5 ha of deforestation warnings not detected by the optical DETER in the same period, and 3317.4 ha of relatively old deforestation not previously detected by PRODES. These additional warnings can be of uttermost importance, particularly in areas that are being severely affected by the expansion of the deforestation fronts with high cloud cover, such as the BR-319 [46]. Illegal mining spots, which normally expand during the rainy season, usually are not readily detected with optical imagery. DETER-R warnings can be of great help in this case as well.

## 6. Conclusions

This study presented the DETER-R system early and current routines, as well as the results generated in its prototype phase and after its first year of operation. The proposed system, designed to support the optical DETER in issuing forest disturbance warnings during periods of constant cloud cover in the Brazilian Amazon, generated very few false positives results (less than 0.5% of the detected polygons as false positives). DETER-R were able to provide additional areas of deforestation warnings to monitoring teams, not detected by its optical counterpart DETER in the same period, as well as areas not previously detected by PRODES, with very little need for human intervention. Our results also show that the contributions of DETER-R are more expressive during the rainy season.

We also explored the caveats of the system, such as the delay from the first detection and the issuing of the warning, caused by the need of confirmation of the disturbance, the source of the observed disagreements, and general caveats when compared to other NRT systems in operations. These results suggest that the actual parametrization of the DETER-R system is provoking a high rate of omissions, with approximately half of the deforested areas not being detected by the system. This kind of configuration impedes, for example, the use of our detection results as a deforestation accounting system for a particular area and period. It is important to note that this is a consequence of a design option on a particular application, and not a system flaw by itself. Ultimately, it is up to the user of the system to set the detection parameters (namely the minimum mapping unit and the false alert ratio) most adequate to the studied problem.

These findings, together with the analysis herein presented, highlight the usefulness of DETER-R within the Brazilian monitoring of Amazon, as well as indicate important paths for the improvement of DETER-R in the future, such as enlarging the feature space of the algorithm to add textural or precipitation information, or to explore the possibilities of deep learning both to increase the system speed, as well to better identify subclasses of forest disturbance. Furthermore, we believe that DETER-R might be applied on other tropical regions, constituting an important tool for forest disturbance detection and control.

**Author Contributions:** Conceptualization, J.D., M.S.R. and C.A.A.; methodology, J.D.; software, J.D., A.F.A.C. and L.E.P.M.; validation, C.B.Q., D.R.V.M. and A.P.B.; resources, C.A.A.; writing—original draft preparation, J.D. and M.S.R.; writing—review and editing, J.D., M.S.R., S.J.S.S. and Y.E.S.; supervision, C.A.A., L.E.P.M., S.J.S.S. and Y.E.S.; project administration, C.A.A. All authors have read and agreed to the published version of the manuscript.

## References

1. Harris, N.L.; Gibbs, D.A.; Baccini, A.; Birdsey, R.A.; de Bruin, S.; Farina, M.; Fatoyinbo, L.; Hansen, M.C.; Herold, M.; Houghton, R.A.; et al. Global maps of twenty-first century forest carbon fluxes. *Nat. Clim. Chang.* **2021**, *11*, 234–240. [CrossRef]
2. Gatti, L.V.; Basso, L.S.; Miller, J.B.; Gloor, M.; Gatti Domingues, L.; Cassol, H.L.; Tejada, G.; Aragão, L.E.; Nobre, C.; Peters, W.; et al. Amazonia as a carbon source linked to deforestation and climate change. *Nature* **2021**, *595*, 388–393. [CrossRef] [PubMed]
3. WRI. *Global Forest Review*; WRI: Washington, DC, USA, 2021.
4. Assunção, J.; Gandour, C.; Rocha, R. DETERring Deforestation in the Amazon: Environmental Monitoring and Law Enforcement; Climate Policy Initiative Report. 2019. Available online: https://www.climatepolicyinitiative.org/working-papers/deterring-deforestation-in-the-amazon-environmental-monitoring-and-law-enforcement/ (accessed on 1 May 2021).
5. Finer, B.M.; Novoa, S.; Weisse, M.J.; Petersen, R.; Mascaro, J.; Souto, T.; Stearns, F.; Martinez, R.G. Combating deforestation: From satellite to intervention. *Science (80-)* **2018**, *360*, 1303–1305. [CrossRef] [PubMed]
6. Diniz, C.G.; Souza, A.A.D.A.; Santos, D.C.; Dias, M.C.; Luz, N.C.D.; Moraes, D.R.V.D.; Maia, J.S.A.; Gomes, A.R.; Narvaes, I.D.S.; Valeriano, D.M.; et al. DETER-B: The New Amazon Near Real-Time Deforestation Detection System. *IEEE J. Sel. Top. Appl. Earth Obs. Remote Sens.* **2015**, *8*, 3619–3628. [CrossRef]
7. Doblas, J.; Shimabukuro, Y.; Sant'anna, S.; Carneiro, A.; Aragão, L.; Almeida, C. Optimizing near real-time detection of deforestation on tropical rainforests using Sentinel-1 data. *Remote Sens.* **2020**, *12*, 3922. [CrossRef]
8. Weisse, M.J.; Noguerón, R.; Eduardo, R.; Vicencio, V.; Castillo Soto, D.A. *Use of Near-Real-Time Deforestation Alerts: A Case Study from Peru*; Technical Report; WRI.ORG: Washington, DC, USA, 2019.
9. Danklmayer, A.; Doring, B.R.J.; Schwerdt, M.; Chandra, M. Assessment of atmospheric propagation effects in SAR images. *IEEE Trans. Geosci. Remote Sens.* **2009**, *47*, 3507–3518. [CrossRef]
10. Watanabe, M.; Koyama, C.N.; Hayashi, M.; Nagatani, I.; Shimada, M. Early-stage deforestation detection in the tropics with L-band SAR. *IEEE J. Sel. Top. Appl. Earth Obs. Remote Sens.* **2018**, *11*, 2127–2133. [CrossRef]
11. Watanabe, M.; Koyama, C.N.; Hayashi, M.; Nagatani, I.; Tadono, T.; Shimada, M. Refined algorithm for forest early warning system with ALOS-2/PALSAR-2 ScanSAR data in tropical forest regions. *Remote Sens. Environ.* **2021**, *265*, 112643. [CrossRef]
12. Reiche, J.; Verhoeven, R.; Verbesselt, J.; Hamunyela, E.; Wielaard, N.; Herold, M. Characterizing tropical forest cover loss using dense Sentinel-1 data and active fire alerts. *Remote Sens.* **2018**, *10*, 777. [CrossRef]
13. Gorelick, N.; Hancher, M.; Dixon, M.; Ilyushchenko, S.; Thau, D.; Moore, R. Google Earth Engine: Planetary-scale geospatial analysis for everyone. *Remote Sens. Environ.* **2017**, *202*, 18–27. [CrossRef]
14. Reiche, J.; Mullissa, A.; Slagter, B.; Gou, Y.; Tsendbazar, N.E.; Odongo-Braun, C.; Vollrath, A.; Weisse, M.J.; Stolle, F.; Pickens, A.; et al. Forest disturbance alerts for the Congo Basin using Sentinel-1. *Environ. Res. Lett.* **2021**, *16*, 024005. [CrossRef]
15. Bouvet, A.; Mermoz, S.; Ballère, M.; Koleck, T.; Le Toan, T. Use of the SAR Shadowing Effect for Deforestation Detection with Sentinel-1 Time Series. *Remote Sens.* **2018**, *10*, 1250. [CrossRef]
16. Ballère, M.; Bouvet, A.; Mermoz, S.; Le Toan, T.; Koleck, T.; Bedeau, C.; André, M.; Forestier, E.; Frison, P.L.; Lardeux, C. SAR data for tropical forest disturbance alerts in French Guiana: Benefit over optical imagery. *Remote Sens. Environ.* **2021**, *252*, 112159. [CrossRef]
17. Mermoz, S.; Bouvet, A.; Koleck, T.; Ballère, M.; Le Toan, T. Continuous Detection of Forest Loss in Vietnam, Laos, and Cambodia Using Sentinel-1 Data. *Remote Sens.* **2021**, *13*, 4877. [CrossRef]
18. Greidanus, H.; Alvarez, M.; Santamaria, C.; Thoorens, F.X.; Kourti, N.; Argentieri, P. The SUMO Ship Detector Algorithm for Satellite Radar Images. *Remote Sens.* **2017**, *9*, 246. [CrossRef]
19. Xu, Z.; Zhang, H.; Wang, Y.; Wang, X.; Xue, S.; Liu, W. Dynamic detection of offshore wind turbines by spatial machine learning from spaceborne synthetic aperture radar imagery. *J. King Saud Univ.-Comput. Inf. Sci.* **2022**, *34*, 1674–1686. [CrossRef]
20. Touzi, R.; Lopes, A.; Bousquet, P. A statistical and geometrical edge detector for SAR images. *IEEE Trans. Geosci. Remote Sens.* **1988**, *26*, 764–773. [CrossRef]
21. Sano, E.E.; Rizzoli, P.; Koyama, C.N.; Watanabe, M.; Adami, M.; Shimabukuro, Y.E.; Bayma, G.; Freitas, D.M. Comparative analysis of the global forest/non-forest maps derived from sar and optical sensors. Case studies from brazilian amazon and cerrado biomes. *Remote Sens.* **2021**, *13*, 367. [CrossRef]
22. Monitoramento do Desmatamento da Floresta Amazônica Brasileira por Satélite. 2022. Available online: http://www.obt.inpe.br/OBT/assuntos/programas/amazonia/prodes (accessed on 2 May 2022).

23. Martone, M.; Rizzoli, P.; Wecklich, C.; González, C.; Bueso-Bello, J.L.; Valdo, P.; Schulze, D.; Zink, M.; Krieger, G.; Moreira, A. The global forest/non-forest map from TanDEM-X interferometric SAR data. *Remote Sens. Environ.* **2018**, *205*, 352–373. [CrossRef]

24. Melack, J.M.; Hess, L.L. Remote Sensing of the Distribution and Extent of Wetlands in the Amazon Basin. In *Amazonian Floodplain Forests: Ecophysiology, Biodiversity and Sustainable Management*; Junk, W.J., Piedade, M.T.F., Wittmann, F., Schöngart, J., Parolin, P., Eds.; Springer: Dordrecht, The Netherlands, 2011; pp. 43–59. [CrossRef]

25. Rennó, C.D.; Novo, E.M.; Banon, L.C. Correção geométrica da máscara de áreas alagáveis da bacia amazônica. In Proceedings of the Anais XVI Simpósio Brasileiro de Sensoriamento Remoto, Foz do Iguaçu, Brasil, 13–18 April 2013; pp. 5507–5514.

26. Diretoria de Geociências (IBGE/DGC). *Base temática Vetorial 1:250.000—Brasil—Geomorfologia – Área*; Technical Report; Coordenação de Recursos Naturais e Estudos Ambientais—CREN (IBGE): Rio de Janeiro, Brazil, 2018.

27. Vollrath, A.; Mullissa, A.; Reiche, J. Angular-based radiometric slope correction for Sentinel-1 on google earth engine. *Remote Sens.* **2020**, *12*, 1867. [CrossRef]

28. Quegan, S.; Yu, J.J. Filtering of multichannel SAR images. *IEEE Trans. Geosci. Remote Sens.* **2001**, *39*, 2373–2379. [CrossRef]

29. Doblas, J.; Frery, A.C.; Sant'Anna, S.J.S.; Carneiro, A.; Shimabukuro, Y.E. Assessment of Nonlocal Means Stochastic Distances Speckle Reduction for SAR Time Series. In Proceedings of the 2021 IEEE International Geoscience and Remote Sensing Symposium IGARSS, Brussels, Belgium, 11–16 July 2021; pp. 3265–3268. [CrossRef]

30. Lee, J.S. Refined filtering of image noise using local statistics. *Comput. Graph. Image Process.* **1981**, *15*, 380–389. [CrossRef]

31. Lee, J.S. Speckle analysis and smoothing of synthetic aperture radar images. *Comput. Graph. Image Process.* **1981**, *17*, 24–32. [CrossRef]

32. Benninga, H.J.F.; van der Velde, R.; Su, Z. Impacts of Radiometric Uncertainty and Weather-Related Surface Conditions on Soil Moisture Retrievals with Sentinel-1. *Remote Sens.* **2019**, *11*, 2025. [CrossRef]

33. Doblas, J.; Carneiro, A.; Shimabukuro, Y.; Sant'anna, S.; Aragão, L.; Pereira, F.R. Stabilization of sentinel-1 sar time-series using climate and forest structure data for early tropical deforestation detection. *ISPRS Ann. Photogramm. Remote Sens. Spat. Inf. Sci.* **2020**, *5*, 89–96. [CrossRef]

34. Nunes, M.H.; Camargo, J.L.C.; Vincent, G.; Calders, K.; Oliveira, R.S.; Huete, A.; Mendes de Moura, Y.; Nelson, B.; Smith, M.N.; Stark, S.C.; et al. Forest fragmentation impacts the seasonality of Amazonian evergreen canopies. *Nat. Commun.* **2022**, *13*, 1–10. [CrossRef]

35. Delignette-Muller, M.L.; Dutang, C. fitdistrplus: An R Package for Fitting Distributions. *J. Stat. Softw.* **2015**, *64*, 1–34. doi: [CrossRef]

36. Maurano, L.E.; Adami, M. Ferramentas Web-Gis para avaliar exatidão de mapeamento de uso e cobertura da terra no Cerrado brasileiro. In Proceedings of the Anais XVIII Simpósio Brasileiro de Sensoriamento Remoto, São Paulo, Brazil, 28–31 May 2017 ; pp. 462–469.

37. Alencar, A.; Silvestrini, R.; Gomes, J.; Savian, G. *Amazon in Flames: The New and Alarming Level of Deforestation in the Amazon*; Technical Report 9; IPAM: Brasília, Brazil, 2022.

38. Hansen, M.C.; Krylov, A.; Tyukavina, A.; Potapov, P.V.; Turubanova, S.; Zutta, B.; Ifo, S.; Margono, B.; Stolle, F.; Moore, R. Humid tropical forest disturbance alerts using Landsat data. *Environ. Res. Lett.* **2016**, *11*, 034008. [CrossRef]

39. Doblas, J.; Lima, L.; Mermoz, S.; Bouvet, A.; Reiche, J.; Watanabe, M.; Sant'Anna, S.; Shimabukuro, Y. Inter-comparison of optical and SAR-based forest disturbance warning systems in the Amazon shows the potential of combined SAR-optical monitoring. *Int. J. Remote Sens.* **2022**, *submitted*.

40. Pickens, A.; Hansen, M.; Adusei, B.; Potapov, P. *Sentinel-2 Forest Loss Alerts*; WRI.ORG: Washington, DC, USA, 2020.

41. Doblas, J.; Carneiro, A.; Shimabukuro, Y.; Sant'Anna, S.; Aragão, L. Assessment of rainfall influence on sentinel-1 time series on amazonian tropical forests aiming deforestation detection improvement. In Proceedings of the 2020 IEEE Latin American GRSS & ISPRS Remote Sensing Conference (LAGIRS), Santiago, Chile, 22–27 March 2020; pp. 397–402. [CrossRef]

42. Silva, C.A.; Guerrisi, G.; Del Frate, F.; Sano, E.E. Near-real time deforestation detection in the Brazilian Amazon with Sentinel-1 and neural networks. *Eur. J. Remote Sens.* **2022**, *55*, 129–149. [CrossRef]

43. Zhu, X.X.; Montazeri, S.; Ali, M.; Hua, Y.; Wang, Y.; Mou, L.; Shi, Y.; Xu, F.; Bamler, R. Deep Learning Meets SAR: Concepts, models, pitfalls, and perspectives. *IEEE Geosci. Remote Sens. Mag.* **2021**, *9*, 143–172. [CrossRef]

44. Ortega Adarme, M.; Doblas Prieto, J.; Queiroz Feitosa, R.; De Almeida, C.A. Improving Deforestation Detection on Tropical Rainforests Using Sentinel-1 Data and Convolutional Neural Networks. *Remote Sens.* **2022**, *14*, 3290. [CrossRef]

45. Hethcoat, M.G.; Carreiras, J.M.B.; Bryant, R.G.; Quegan, S.; Edwards, D.P. Combining Sentinel-1 and Landsat 8 Does Not Improve Classification Accuracy of Tropical Selective Logging. *Remote Sens.* **2022**, *14*, 179. [CrossRef]

46. Ferrante, L.; De Andrade, M.B.T.; Leite, L.; Silva, C.A.; Lima, M.; Coelho, M.G.; Da Silva Neto, E.C.; Campolina, D.; Carolino, K.; Diele-Viegas, L.M.; et al. Brazils highway BR-319: The road to the collapse of the Amazon and the violation of indigenous rights. *Erde* **2021**, *152*, 65–70. [CrossRef]